Determination of Resonance Raman Cross-Sections for Use in Biological SERS Sensing with Femtosecond Stimulated Raman Spectroscopy

ARTICLE *in* ANALYTICAL CHEMISTRY · JUNE 2014

Impact Factor: 5.64 · DOI: 10.1021/ac501701h · Source: PubMed

3 AUTHORS, INCLUDING:

Renee Frontiera
University of Minnesota Twin Cities
20 PUBLICATIONS **963** CITATIONS

analytical chemistry

Article

pubs.acs.org/ac

Determination of Resonance Raman Cross-Sections for Use in Biological SERS Sensing with Femtosecond Stimulated Raman Spectroscopy

W. Ruchira Silva, Emily L. Keller, and Renee R. Frontiera*

Department of Chemistry, University of Minnesota, Minneapolis, Minnesota 55455, United States

Supporting Information

ABSTRACT: Surface-enhanced Raman spectroscopy (SERS) is a promising technique for *in vivo* bioanalyte detection, but accurate characterization of SERS biosensors can be challenging due to difficulties in differentiating resonance and surface enhancement contributions to the Raman signal. Here, we quantitate the resonance Raman cross-sections for a commonly used near-infrared SERS dye, 3,3′-diethylthiatricarbocyanine (DTTC). It is typically challenging to measure resonance Raman cross-sections for fluorescent dye molecules due to the overwhelming isoenergetic fluorescence signal. To overcome this issue, we used etalon-based femtosecond stimulated Raman spectroscopy, which is intrinsically designed to acquire a stimulated Raman signal without strong fluorescence or interference from signals resulting from other four-wave mixing pathways. Using this technique, we found that the cross-sections for most of the resonantly enhanced modes in DTTC exceed 10^{-25} cm^2/molecule. These cross-sections lead to high signal magnitude SERS signals from even weakly enhancing SERS substrates, as much of what appears to be a SERS signal is actually coming from the intrinsically strong resonance Raman signal. Our work will lead to a more accurate determination of SERS enhancement factors and SERS substrate characterization in the biologically relevant near-infrared region, ultimately leading to a more widespread use of SERS for biosensing and bioimaging applications.

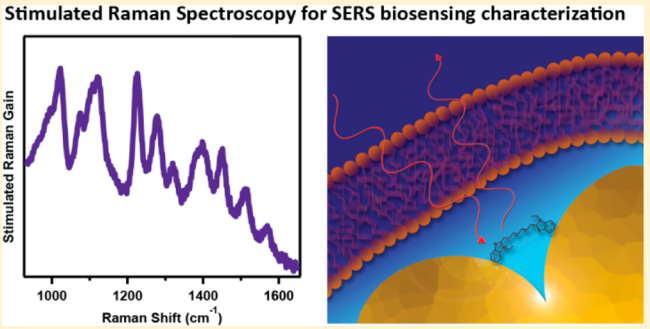

Surface-enhanced Raman spectroscopy (SERS) is an ideal technique for sensing a wide variety of analytes in various media, as it is a label-free, highly sensitive method which provides chemical structural information with rapid sample preparation and detection steps.[1−3] SERS sensors are most effective when substrates are optimized for both strong surface enhancement as well as high overall signal magnitudes. The latter goal is typically achieved by using resonant dyes to tag or characterize SERS substrates. However, it can then be challenging to differentiate resonance and surface enhancement effects, as resonance Raman cross-sections for many dye molecules have not been measured due to overwhelming fluorescence background signals.

In complex biological media, the competition between Raman scattering and elastic scattering has led to widespread development of SERS sensors optimized in the near-infrared region. This is due to the fact that irradiation in the ∼700 to 900 nm region of the electromagnetic spectrum minimizes unwanted processes such as elastic scattering, autofluorescence, and absorption by hemoglobin and water molecules,[4−8] leading to the largest optical penetration depths and typically the highest magnitude SERS signals. At these wavelengths, 3,3′-diethylthiatricarbocyanine (DTTC) is a frequently used SERS analyte as it is readily available, biocompatible, and binds well to gold plasmonic substrates.[9−18]

A careful quantitation of the enhancement factor for a given SERS substrate is critical when evaluating materials for biological sensing but can be challenging due to the numerous assumptions and uncertainties which contribute to the enhancement factor calculation.[19,20] SERS enhancement factors determine by how much a given plasmonic material boosts the Raman signal, ideally by taking the ratio of the Raman signal magnitude with and without the SERS substrate. In practice, a direct comparison is typically not possible, due to factors such as analyte fluorescence or undetectably weak Raman signals in the absence of a plasmonic material. Other challenges can include accurately calculating surface area coverage on a given substrate and accounting for changes in plasmon resonances during the course of the measurements done at high laser power. As a result, enhancement factors can vary by many orders of magnitude for a given substrate depending on the assumptions made in the calculation.

A particular challenge for enhancement factor calculations is the lack of resonance Raman cross-sections for the fluorescent dyes used for resonance SERS measurements. In normal Raman measurements of fluorescent molecules, the fluores-

Received: May 7, 2014
Accepted: June 29, 2014

dx.doi.org/10.1021/ac501701h | *Anal. Chem.* XXXX, XXX, XXX−XXX

cence of the free dye in solution makes determination of resonance cross-sections extremely challenging, as the isoenergetic fluorescence background greatly overwhelms the much smaller Raman signal. However, in a SERS measurement, the plasmon rapidly quenches the molecular excited state, essentially eliminating fluorescence. The large absorption cross-section and strong polarizibility of dye molecules thus makes them excellent candidates for large SERS signal magnitudes, although the lack of resonance Raman cross-section measurements hinders accurate determination of enhancement factors. Recently, two novel approaches to measuring Raman cross-sections of fluorescent molecules using a well-characterized normal Raman setup have been presented,[21,22] but these have not been applied to the near-infrared regime where silicon-based detectors are significantly noisier and less efficient. A careful determination of resonance Raman cross-sections for the near-infrared dyes used in developing and characterizing SERS substrates for biological sensing is thus urgently needed.

Stimulated Raman spectroscopy (SRS) provides a quantitative method for determining resonance Raman cross-sections of fluorescent molecules. It is nearly free from background fluorescence as the generated signal is coherent and only a small solid angle of scattered light is collected. There are several approaches to using SRS for quantitative measurements. In most forms of SRS, two narrowband laser pulses, typically picoseconds or nanoseconds in duration, are used for Raman pump and probe. This requires that one of the laser beams be scanned in wavelength in order to build up a complete Raman spectrum. In coherent anti-Stokes Raman spectroscopy (CARS), there are multispectral approaches which permit the acquisition of a broadband spectrum, but interference from nonlinear background signals typically leads to dispersive Raman lineshapes. Femtosecond stimulated Raman spectroscopy (FSRS) is a logical choice for quantitative Raman cross-section measurements as it is capable of rapid acquisition of a high resolution broadband spectrum and is compatible with fluorescent molecules. In a FSRS experiment, a picosecond Raman pump pulse and femtosecond probe pulse combine to give the broadband stimulated Raman signal with high spectral resolution.[23,24]

FSRS has previously been used to measure the resonance Raman cross-section of rhodamine 6G,[25] which has proven extremely useful for quantitation of SERS enhancement factors at the 532 nm excitation wavelength. In the biologically relevant near-infrared regime, the resonance FSR spectrum of DTTC has been measured but not quantified.[26] In previous FSRS experiments, the Raman pump pulse temporal profile had a Gaussian pulse shape, which meant that ∼50% of the Raman pump pulse power was used for electronic excitation prior to the arrival of the probe. This results in significant baseline issues and background features due to the interference of other four-wave mixing processes such as stimulated emission.[27]

Here, we utilize an etalon-based FSRS system to quantitate DTTC resonance Raman cross-sections. The etalon results in a Raman pump pulse that minimizes electronic excitations in the sample that might occur temporally before the Raman process is initiated, giving a greatly reduced background from stimulated emission and other interfering processes.[28] We find that the cross-sections are greater than 10^{-25} cm^2/molecule, and SERS signals from DTTC can be readily obtained with very weakly enhancing plasmonic substrates. This work will help significantly in correctly characterizing SERS substrate enhancement factors from a variety of substrates with near-infrared plasmonic behavior, leading to increased quantitative SERS applications in biological sensing.

EXPERIMENTAL SECTION

Femtosecond Stimulated Raman Spectroscopy. FSRS data were taken on a newly constructed optical table. The 4.4 W, 1 kHz fundamental output (Coherent Libra-F-1K-HE) is split to generate the beams necessary for stimulated Raman experiments. The 800 nm Raman pump pulse is generated by passing 415 mW through a custom etalon (TecOptics) to generate a picosecond pulse which decays exponentially with time. This pulse passes through a telescope for beam diameter optimization and manual retroreflector stage for time delay measurements. The near-infrared broadband femtosecond probe pulse is created by continuum generation in sapphire, utilizing 2.5 mW of the fundamental output. This beam passes through an RG830 filter (Thorlabs) to reduce the fundamental intensity and is compressed with fused silica prisms. Both pulses are focused noncollinearly on the sample with a 10 cm focal length lens. Raman pump powers at the sample were varied from 100 μW to 5000 μW, with a 90:10 beam diameter of 150 μm in both dimensions. The probe power was kept constant at 6 μW, with a beam diameter of 40 μm in both dimensions. The probe is collimated after the sample with a 10 cm lens. Both beams are horizontally polarized, and no polarization optics were placed before the spectrograph.

Our system utilizes a Fabry−Perot etalon to minimize contribution from stimulated emission and other four-wave mixing pathways which may occur on resonance when Raman pump photons are incident on the sample prior to the arrival of the probe pulse. Our etalon was designed with a reflectivity of 98.5 ± 0.5% and a parallel spacing of 24 μm. The free spectral range is 230 cm^{-1}, resulting in a high finesse etalon with a spectral bandwidth of ∼2.3 cm^{-1}. Ref 28 directly compares etalon and Gaussian pulse generation methods for use in FSRS. As the etalon has zero electric field prior to the arrival of the probe pulse, electronic excitation is minimized. In FSRS, the Raman amplitude is primarily determined by the Raman pump field amplitude at the time of probe overlap.

The detection system is similar to those used previously for FSRS.[24] A stimulated Raman signal is generated collinearly with the probe, making alignment straightforward. The probe and signal are directed into a 1/3 m spectrograph (Princeton Instruments 2300i), dispersed on a 600 gr/mm grating blazed at 750 nm, and focused onto a CCD array detector (Princeton Instruments PIXIS 100F). The grating is oriented for maximum diffraction efficiency of our horizontally polarized beams. An RG1000 filter (Thorlabs) is placed before the spectrograph to compensate for low silicon detector efficiency at long wavelengths. Data collection is enabled through home-written Labview software which acquires triggered spectra at the 1 kHz repetition rate of the laser. All spectra are presented as Raman gain, in that a single Raman-pump-on spectrum is divided by the subsequent Raman-pump-off spectrum. To this end, a chopper (Thorlabs MC2000) is placed in the Raman pump path and chops the spectra at half the laser repetition rate, ensuring that the Raman pump pulse is present on the sample for every other spectrum. A home-built flip-flop circuit ensures that the detector receives the appropriate triggering signals with respect to the chopper state. Acquisition times for these experiments ranged from 5−10 min per spectrum. As the spectra are intrinsically normalized to the probe pulse power at

dx.doi.org/10.1021/ac501701h | Anal. Chem. XXXX, XXX, XXX−XXX

each wavelength, no detector instrument response function was needed.

Sample Preparation. DTTC iodide and HPLC grade methanol (Sigma-Aldrich) were used as received. Samples were placed in a 2-mm-thick glass cuvette (Starna cells), and all samples were checked for degradation after experiments by optical absorption spectroscopy (Ocean Optics 4000+). Gold nanoparticles were synthesized for SERS through the standard citrate reduction method.[29] A total of 6.1 mg of $AuCl_3 \cdot 3H_2O$ dissolved in 61 mL of H_2O were mixed with 3.9 mg of sodium citrate dihydrate dissolved in 3.9 mL of H_2O under heat and stirring. The sample for SERS consisted of 500 μL of as-synthesized gold particles, 500 μL of 10 mM NaCl in water, and 100 μL of 7.34×10^{-6} M DTTC in methanol. The sample was allowed to aggregate for 10 min before the SERS measurement, and the measurement was taken with a 2-mm-path-length cuvette.

SERS. The CW surface-enhanced Raman spectrum was taken on a home-built Raman spectrometer. A horizontally polarized 785 nm laser (Innovative Photonics) illuminates the sample through an Olympus 20× LWD objective, with a power at the sample of 30.6 mW. Backscattered Raman light is collected through a 70:30 beamsplitter (CVI Laser). Raman scattered light is focused onto a spectrograph (Princeton Instruments 2500i) and dispersed onto a CCD (Princeton Instruments PIXIS 400BX) by a 600 gr/mm grating blazed at 750 nm. No polarization optics were used in the setup, and the spectrograph grating grooves were oriented perpendicular to our excitation beam polarization. Spectra are scaled by a detector response function measured with a standard lamp (Princeton Instruments Intellical). SERS enhancement factors were determined by first calculating the Raman system response with a straight methanol blank in a matched cuvette. We then determined the DTTC SERS signal by measuring the peak area and using the appropriate cross-section calculated from the FSR data. This was compared to the known DTTC concentration in the SERS sample to obtain the enhancement factor. This method assumes that all DTTC molecules in our 10^{-7} M solution contribute to the SERS signal and that the system response does not change as a result of Mie scattering from the particles. Due to these uncertainties, we report enhancement factors with significance only to the tens unit.

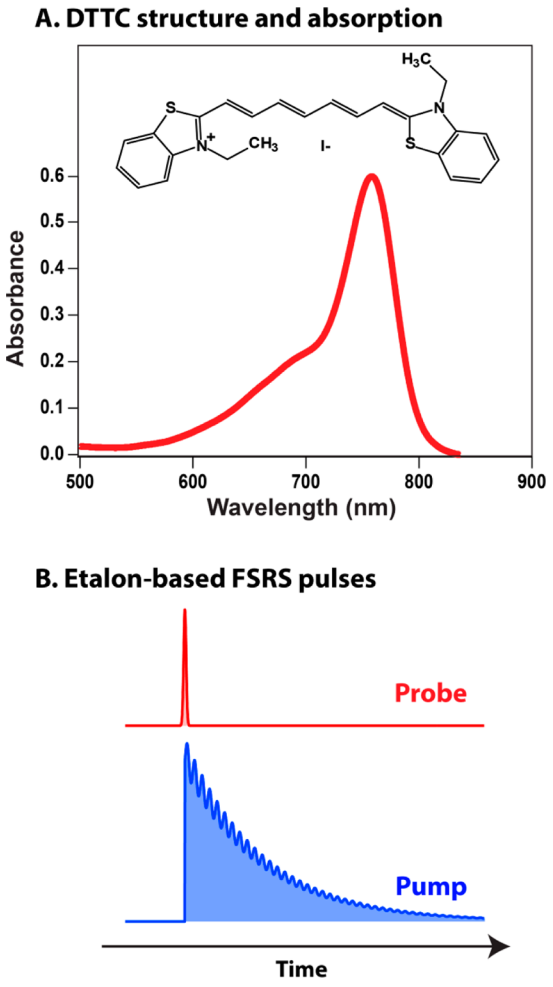

Figure 1. (A) Structure and absorbance spectrum of 3,3′-diethylthiatricarbocyanine (DTTC) iodide in methanol. (B) Temporal profiles of the two pulses used for femtosecond stimulated Raman spectroscopy (FSRS) experiments. A stimulated Raman signal is generated through the interaction of the broadband femtosecond probe pulse and the 800 nm picosecond pump pulse. The pump pulse is generated with an etalon, giving rise to the distinctive exponential decay profile. We observe periodic modulations of the intensity due to a varying number of reflections of the pulse packet in the etalon.

RESULTS AND DISCUSSION

DTTC is a near-infrared absorbing dye molecule commonly used for resonance SERS experiments in the biological water window. The chemical structure and absorption spectrum of DTTC iodide are shown in Figure 1, along with temporal depictions of the two pulses used for our FSRS experiment. The red edge of the DTTC absorption spectrum is resonant with our 800 nm pump pulse. Attempts at measuring the resonance Raman spectrum on a conventional Raman spectrometer resulted in a broad fluorescence background with no discernible Raman peaks, as expected. The temporal depiction of the pulses used in our etalon-based FSRS system consists of a femtosecond probe pulse with Gaussian temporal shape and a picosecond pump pulse from the etalon. This pulse displays a sharp rise at time zero, followed by an exponential decay. Very few pump photons interact with the sample before the probe pulse arrival, leading to minimal excited state generation. As the picosecond pump pulse is created from a femtosecond pulse repeatedly reflected in the etalon, we do see an oscillatory feature in the pump amplitude corresponding to the path-length between the mirrors, as depicted in Figure 1b.

In Figure 2, we show the resonance FSR spectra of DTTC in methanol. It is clear that the stimulated Raman process is sufficiently free from background fluorescence to easily resolve the resonant Raman peaks of DTTC. There is a small but broad background signal from other four wave mixing pathways such as stimulated fluorescence or resonant Rayleigh scattering.[27]

Unlike FSR spectra of DTTC taken with Raman pump pulses which are Gaussian in duration,[26] the use of an etalon prevents the appearance of dispersive lineshapes on resonance, and peaks are easily fit by Lorentzian lineshapes. The fit in Figure 2 shows the 12 major peaks of DTTC fit with Lorentzian functions on top of a broad polynomial background. The frequencies, amplitudes, and widths of all peaks were freely varied in the fitting. The oscillatory feature in the etalon temporal profile should result in an oscillatory baseline feature in the spectrum, but this is fortunately below our signal-to-noise ratio and is not detected.

dx.doi.org/10.1021/ac501701h | Anal. Chem. XXXX, XXX, XXX−XXX

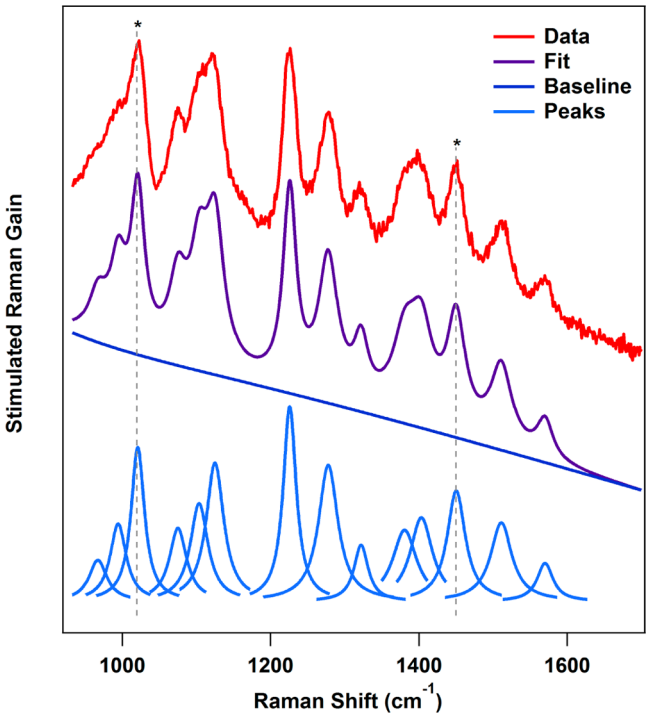

Figure 2. FSR spectrum of DTTC in methanol taken with an 800 nm Raman pump pulse. The spectrum (red) can be fit (purple) by a polynomial baseline (dark blue) with Lorentzian peaks (light blue). Solvent peaks are marked with an asterisk.

Nonlinear processes like FSRS are likely to saturate under high intensity femtosecond pulses,[30] which could lead to erroneously low cross-section measurements. In FSRS, the signal should be linear in Raman pump power for quantitative measurements.[31] Since the stimulated Raman spectra are normalized by the probe power, the Raman gain signals are independent of probe power. In Figure 3, we present the Raman pump power dependence of our DTTC FSR spectra. The nonlinear regime is easily achievable with our experimental setup, the onset of which occurs around 600 μW. Accordingly, we utilized powers of 300 μW for all measurements, well within the linear regime. The power dependence remained linear for higher DTTC concentrations (see Supporting Information).

Like many nonlinear optical processes, FSR spectra can include contributions from background signals such as stimulated emission or fluorescence. In Figure 4, we show that the use of an etalon-based Raman pump pulse can reduce the background contribution, by preventing electronic excitation which occurs before the initiation of the Raman process. By changing the time delay between the Raman pump and probe pulse, we see that the Raman process is at maximum intensity when the pulses are temporally overlapped at their peak intensities. As the probe pulse is delayed relative to the peak of the Raman pump pulse, we see increased contribution of the stimulated emission background, due to electronic excitation occurring before the probe pulse arrival. The spectra in Figure 2 were taken at a time delay of 0 fs, with only minimal contribution from other four wave mixing processes. Figure 4 also shows oscillatory features as a function of time delay, as a result of the pulsed nature of the etalon.

Having proven that we are in a linear power regime and that background signals are minimized, we calculated the resonant Raman cross-section of DTTC using the data presented in

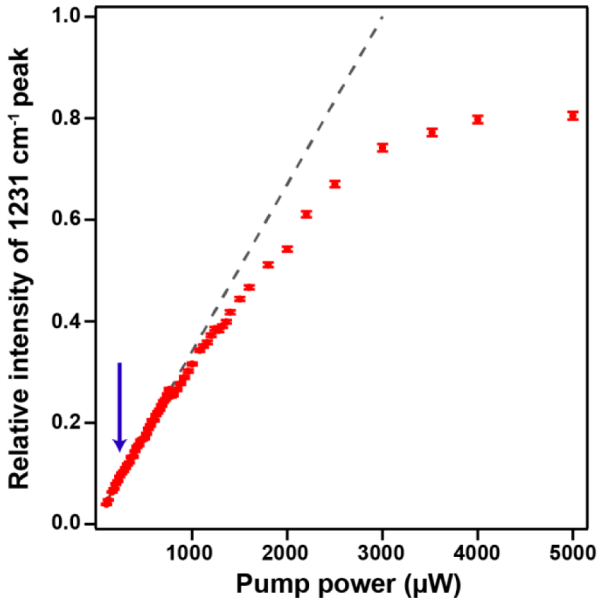

Figure 3. Raman pump power dependence of DTTC Raman signal taken with 800 nm etalon-based FSRS. The signal rapidly saturates at high pump powers, but the linear regime is easily achievable below ~600 μW. All cross-section data were taken at powers of 300 μW, as indicated by the arrow. The concentration of DTTC in methanol was 5.1×10^{-5} M.

Figure 2. We used the 1030 cm^{-1} peak of methanol as an internal standard, for which the differential cross-section is 2.1×10^{-31} cm^2/sr at 785 nm.[32] This was converted to an absolute cross-section using eq 1:[33]

$$\sigma_R = \frac{8\pi}{3}\frac{(1+2\rho)}{(1+\rho)}\frac{\partial\sigma}{\partial\Omega_{\parallel\perp}} \quad (1)$$

where σ_R = absolute Raman cross-section, ρ = depolarization ratio, and $(\partial\sigma)/(\partial\Omega_{\parallel\perp})$ is the differential cross-section measured in both the parallel and perpendicular directions. We used the measured depolarization ratio for methanol's CO stretch of 0.21.[34] We obtained the Lorentzian peak areas from fitting and compared the integrated peak areas to that of the methanol standard. The values for absolute Raman cross-sections of DTTC are listed in Table 1. Standard deviations were calculated by measuring and fitting spectra from three different DTTC samples. The cross-sections for many of the modes exceed 10^{-25} cm^2/molecule. These cross-section values indicate that much of the near-infrared SERS signal from DTTC may actually come from resonance contributions rather than SERS enhancement.

As an application of the accurate resonance Raman cross-section measurements of DTTC, we examined the resonance SERS behavior of this analyte on aggregated gold colloids in solution. These simple SERS complexes provided excellent SERS signal magnitudes when excited with a resonant 785 nm laser, as shown in Figure 5. The concentration of DTTC in this sample was kept low at 667 nM. Some of the frequencies shift by several wavenumbers in the SERS experiment as compared to the stimulated Raman experiment, as reported in Table 2, which we attribute to molecular interactions with the metal surface. Most notably, the modes seen at 1327 and 1076 cm^{-1} in FSRS shift by 7 and 8 cm^{-1}, respectively, in SERS. These two modes primarily consist of in plane H-wagging character, which are likely to be perturbed by the presence of the gold surface.

dx.doi.org/10.1021/ac501701h | Anal. Chem. XXXX, XXX, XXX–XXX

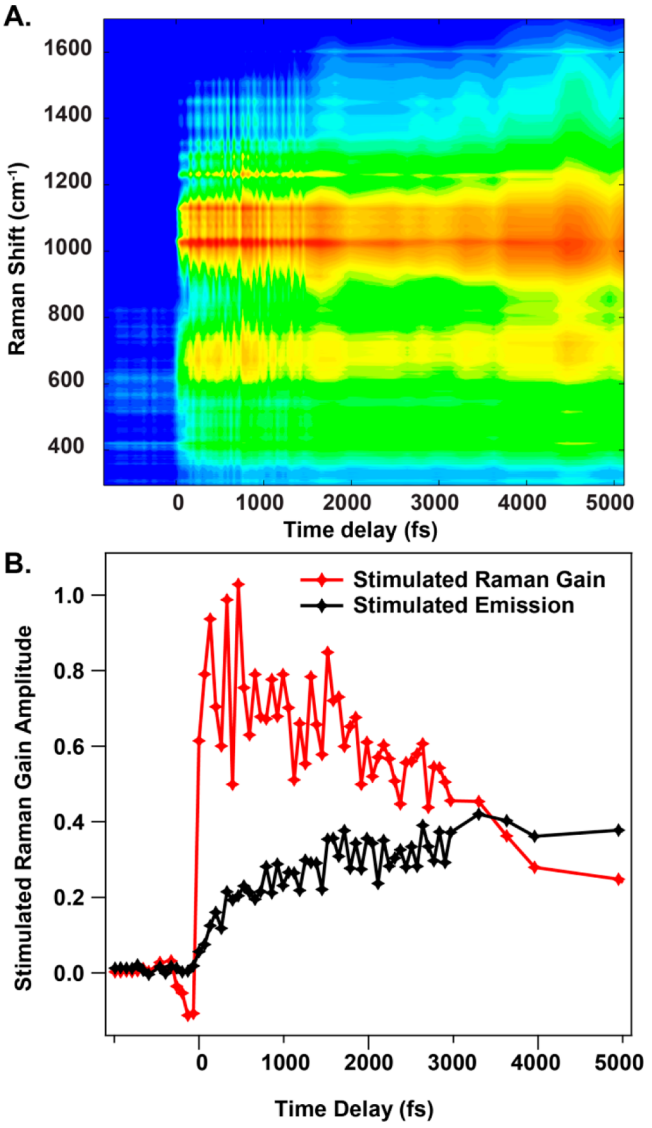

Figure 4. (A) Time delay dependence of DTTC FSR spectra, taken as a function of the delay between the 800 nm pump and probe pulse. Sharp Raman features are clearly visible on a broad background. (B) Intensity of Raman peak at 1231 cm^{-1} and emission signals as a function of time. The stimulated emission feature was measured in clean regions of the spectrum by averaging the signals between 850–875 and 1875–1900 cm^{-1}. The oscillatory features are real and are a function of the etalon. The stimulated emission signal is minimal as compared to Gaussian pulse FSRS systems and is temporally delayed from the peak of the Raman signal.

Four of the modes seen in FSRS are not seen in SERS, of which two are obscured by the relatively larger amplitude methanol peaks in the SER spectrum. However, the majority of the modes are visible and shifted by less than 10 cm^{-1}. Assuming all DTTC molecules contribute to the SERS signal, we calculate enhancement factors for all SERS active modes, which range from 20 to 160, as listed in Table 2. In all experiments, the enhancement factors were less than 3 orders of magnitude, yet the SERS signal was clearly observed with minimal signal averaging. Remarkably, a strong SERS signal is visible with these very weakly enhancing substrates, demonstrating that the main function of the gold nanoparticles in this experiment is to quench the fluorescence, allowing the inherently strong resonance Raman signal to be observed.

Table 1. Resonance Raman Frequencies, Cross-sections, and Standard Deviations for Cross-section Measurements in the Near-infrared Dye DTTC, Taken with an 800 nm Etalon-based FSR Spectrometer

Raman shift (cm^{-1})	resonance Raman cross-section (cm^2/molecule × 10^{-25})	standard deviation (cm^2/molecule × 10^{-25})
974	2.4	0.9
996	4.6	1.2
1076	6.2	1.2
1106	9.6	1.6
1128	11.5	0.3
1229	14.1	2.4
1281	15.1	2.7
1327	4.4	0.5
1384	7.3	0.9
1406	9.2	0.4
1514	7.1	0.8
1572	2.5	0.4

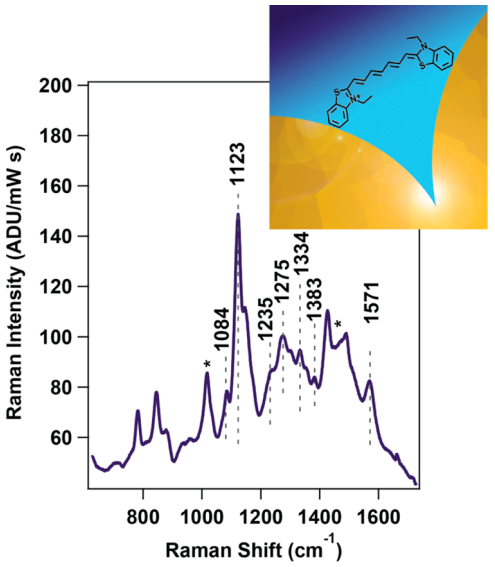

Figure 5. Surface-enhanced Raman spectrum of DTTC on aggregated gold colloids, taken with 785 nm excitation. Raman intensities are plotted in terms of analog to digital units (ADU) and normalized by pump power (in mW) and acquisition time (in seconds) for ease of comparison between other Raman systems. Strong Raman peaks and significantly reduced fluorescence are seen even with only weakly enhancing SERS substrates. Asterisks indicate solvent peaks.

CONCLUSION

The resonance Raman cross-sections determined by our etalon-based femtosecond stimulated Raman spectrometer will significantly impact enhancement factor calculations for SERS substrates optimized for the near-infrared bioimaging window. As resonance Raman cross-sections cannot be measured for fluorescent molecules using standard methods, estimates for these values vary widely. Our measurement of the exact cross-sections eliminates this estimation, which should lead to the development of reproducible, highly enhancing, high signal magnitude SERS sensors in the biologically relevant near-infrared region.

dx.doi.org/10.1021/ac501701h | Anal. Chem. XXXX, XXX, XXX–XXX

Table 2. Correlation between DTTC Modes Measured with 800 nm FSR and 785 nm SER Spectrometers, along with Mode-specific SERS Enhancement Factors

Raman shift (cm^{-1}) from FSRS	Raman shift (cm^{-1}) observed in SERS	SERS enhancement factor
974	weak	
996	MeOH interference	
1076	1084	40
1106	weak	
1128	1123	70
1229	1235	20
1281	1275	50
1327	1334	70
1384	1383	30
1406	MeOH interference	
1514	~1512 (weak)	
1572	1571	160

■ ASSOCIATED CONTENT

Supporting Information

Time-delay dependence of cyclohexane standard and power dependence of FSR spectra at different DTTC concentrations. This material is available free of charge via the Internet at http://pubs.acs.org.

■ AUTHOR INFORMATION

Corresponding Author

*E-mail: rrf@umn.edu. Phone: 612-624-2501. Fax: 612-626-7541.

Author Contributions

The manuscript was written through contributions of all authors. All authors have given approval to the final version of the manuscript.

Notes

The authors declare no competing financial interest.

■ ACKNOWLEDGMENTS

We thank Stephanie Hart (University of Minnesota) for acquisition of the absorption spectrum in Figure 1. This work was supported by startup funding from the University of Minnesota.

■ ABBREVIATIONS

SERS surface-enhanced Raman spectroscopy
DTTC 3,3′-diethylthiatricarbocyanine
FSRS femtosecond stimulated Raman spectroscopy

■ REFERENCES

(1) Willets, K. A.; Van Duyne, R. P. *Annu. Rev. Phys. Chem.* **2007**, *58*, 267−297.
(2) Alvarez-Puebla, R. A.; Liz-Marzan, L. M. *Small* **2010**, *6*, 604−610.
(3) Bantz, K. C.; Meyer, A. F.; Wittenberg, N. J.; Im, H.; Kurtulus, O.; Lee, S. H.; Lindquist, N. C.; Oh, S.-H.; Haynes, C. L. *Phys. Chem. Chem. Phys.* **2011**, *13*, 11551−11567.
(4) Weissleder, R. *Nat. Biotechnol.* **2001**, *19*, 316−317.
(5) Konig, K. *J. Microsc.* **2000**, *200*, 83−104.
(6) Reich, G. *Adv. Drug Delivery Rev.* **2005**, *57*, 1109−1143.
(7) Huang, X. H.; El-Sayed, I. H.; Qian, W.; El-Sayed, M. A. *J. Am. Chem. Soc.* **2006**, *128*, 2115−2120.
(8) Gobin, A. M.; Lee, M. H.; Halas, N. J.; James, W. D.; Drezek, R. A.; West, J. L. *Nano Lett.* **2007**, *7*, 1929−1934.
(9) Qian, X.; Peng, X.-H.; Ansari, D. O.; Yin-Goen, Q.; Chen, G. Z.; Shin, D. M.; Yang, L.; Young, A. N.; Wang, M. D.; Nie, S. *Nat. Biotechnol.* **2008**, *26*, 83−90.
(10) Doering, W. E.; Nie, S. M. *Anal. Chem.* **2003**, *75*, 6171−6176.
(11) Fales, A. M.; Yuan, H.; Vo-Dinh, T. *Langmuir* **2011**, *27*, 12186−12190.
(12) Samanta, A.; Maiti, K. K.; Soh, K.-S.; Liao, X.; Vendrell, M.; Dinish, U. S.; Yun, S.-W.; Bhuvaneswari, R.; Kim, H.; Rautela, S.; Chung, J.; Olivo, M.; Chang, Y.-T. *Angew. Chem., Int. Ed.* **2011**, *50*, 6089−6092.
(13) von Maltzahn, G.; Centrone, A.; Park, J.-H.; Ramanathan, R.; Sailor, M. J.; Hatton, T. A.; Bhatia, S. N. *Adv. Mater.* **2009**, *21*, 3175−3180.
(14) Qian, J.; Jiang, L.; Cai, F.; Wang, D.; He, S. *Biomaterials* **2011**, *32*, 1601−1610.
(15) Jiang, L.; Qian, J.; Cai, F.; He, S. *Anal. Bioanal. Chem.* **2011**, *400*, 2793−2800.
(16) Xiao, M.; Nyagilo, J.; Arora, V.; Kulkarni, P.; Xu, D.; Sun, X.; Dave, D. P. *Nanotechnology* **2010**, *21*, 1−8.
(17) Yuan, H.; Fales, A. M.; Khoury, C. G.; Liu, J.; Vo-Dinh, T. *J. Raman Spectrosc.* **2013**, *44*, 234−239.
(18) Cai, H.; Zhu, J.; Chen, G.; Liu, L.; He, G. S.; Zhang, X. *J. Raman Spectrosc.* **2011**, *42*, 1722−1727.
(19) Le Ru, E. C.; Etchegoin, P. G. *MRS Bull.* **2013**, *38*, 631−640.
(20) Kleinman, S. L.; Frontiera, R. R.; Henry, A.-I.; Dieringer, J. A.; Van Duyne, R. P. *Phys. Chem. Chem. Phys.* **2013**, *15*, 21−36.
(21) Le Ru, E. C.; Schroeter, L. C.; Etchegoin, P. G. *Anal. Chem.* **2012**, *84*, 5074−5079.
(22) Auguie, B.; Reigue, A.; Le Ru, E. C.; Etchegoin, P. G. *Anal. Chem.* **2012**, *84*, 7938−7945.
(23) Kukura, P.; McCamant, D. W.; Mathies, R. A. *Annu. Rev. Phys. Chem.* **2007**, *58*, 461−488.
(24) Frontiera, R. R.; Mathies, R. A. *Laser Photonics Rev.* **2011**, *5*, 102−113.
(25) Shim, S.; Stuart, C. M.; Mathies, R. A. *ChemPhysChem* **2008**, *9*, 697−699.
(26) Kim, H. M.; Kim, H.; Yang, I.; Jin, S. M.; Suh, Y. D. *Phys. Chem. Chem. Phys.* **2014**, *16*, 5312−5318.
(27) Frontiera, R. R.; Shim, S.; Mathies, R. A. *J. Chem. Phys.* **2008**, *129*, 064507.
(28) Hoffman, D. P.; Valley, D.; Ellis, S. R.; Creelman, M.; Mathies, R. A. *Opt. Express* **2013**, *21*, 21685−21692.
(29) Frens, G. *Nat. Phys. Sci.* **1973**, *241*, 20−22.
(30) Lee, J.; Challa, J. R.; McCamant, D. W. *J. Raman Spectrosc.* **2013**, *44*, 1263−1272.
(31) McCamant, D. W.; Kukura, P.; Yoon, S.; Mathies, R. A. *Rev. Sci. Instrum.* **2004**, *75*, 4971−4980.
(32) Le Ru, E. C.; Etchegoin, P. G. *Principles of Surface-Enhanced Raman Spectroscopy and Related Plasmonic Effects*, 1st ed.; Elsevier: Oxford, 2009.
(33) Myers, A. B.; Mathies, R. A. In *Biological Applications of Raman Spectroscopy*; Spiro, T. G., Ed.; John Wiley & Sons, Inc.: Hoboken, NJ, 1987; pp 1−58.
(34) McCamant, D. W.; Kukura, P.; Mathies, R. A. *Appl. Spectrosc.* **2003**, *57*, 1317−1323.